Taylor & Francis
Taylor & Francis Group

BRIEF REPORT

☐ OPEN ACCESS ✓ Check for updates
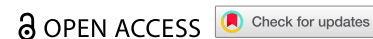
Partial mitochondrial involvement in the antiproliferative and immunostimulatory effects of PT-112

Ruth Soler-Agesta [a,b], Manuel Beltrán-Visiedo [a,c], Ai Sato[a,c], Takahiro Yamazaki[a], Emma Guilbaud[a,c], Christina Y. Yim[b], Maria T. Congenie[b], Tyler D. Ames[b], Alberto Anel [d], and Lorenzo Galluzzi [a,c]

aDepartment of Radiation Oncology, Weill Cornell Medical College, New York, NY, USA; bPromontory Therapeutics, New York, NY, USA; cCancer Signaling and Microenvironment Program, Fox Chase Cancer Center, Philadelphia, PA, USA; dBiochemistry and Molecular and Cell Biology, Aragón Health Research Institute (IIS-Aragón), University of Zaragoza, Zaragoza, Spain

ABSTRACT

PT-112 is a novel small molecule exhibiting promising clinical activity in patients with solid tumors. PT-112 kills malignant cells by inhibiting ribosome biogenesis while promoting the emission of immunostimulatory signals. Accordingly, PT-112 is an authentic immunogenic cell death (ICD) inducer and synergizes with immune checkpoint inhibitors in preclinical models of mammary and colorectal carcinoma. Moreover, PT-112 monotherapy has led to durable clinical responses, some of which persisting after treatment discontinuation. Mitochondrial outer membrane permeabilization (MOMP) regulates the cytotoxicity and immunogenicity of various anticancer agents. Here, we harnessed mouse mammary carcinoma TS/A cells to test whether genetic alterations affecting MOMP influence PT-112 activity. As previously demonstrated, PT-112 elicited robust antiproliferative and cytotoxic effects against TS/A cells, which were preceded by the ICD-associated exposure of calreticulin (CALR) on the cell surface, and accompanied by the release of HMGB1 in the culture supernatant. TS/A cells responding to PT-112 also exhibited eIF2α phosphorylation and cytosolic mtDNA accumulation, secreted type I IFN, and exposed MHC Class I molecules as well as the co-inhibitory ligand PD-L1 on their surface. Acute cytotoxicity and HMGB1 release caused by PT-112 in TS/A cells were influenced by MOMP competence. Conversely, PT-112 retained antiproliferative effects and its capacity to drive type I IFN secretion as well as CALR, MHC Class I and PD-L1 exposure on the cell surface irrespective of MOMP defects. These data indicate a partial involvement of MOMP in the mechanisms of action of PT-112, suggesting that PT-112 is active across various tumor types, including malignancies with MOMP defects.

Introduction

PT-112 is a novel small anticancer agent with immunotherapeutic properties and promising single-agent clinical activity in patients affected by advanced solid tumors of different origin,[1] including (but not limited to) metastatic castration-resistant prostate cancer[2–4] and thymic epithelial tumors.[5,6] In line with this notion, PT-112 has been shown to efficiently arrest the proliferation of and kill a wide panel of human and mouse cancer cell lines,[7–9] with a mechanism of action that appears to involve ribosomal biogenesis inhibition[10] coupled to mitochondrial stress.[8,11] Importantly, PT-112 has also been demonstrated to promote a type of cell death that (in immunocompetent hosts) can elicit the activation of adaptive anticancer immune responses associated with an active effector phase,[9,12] i.e., immunogenic cell death (ICD).[13] Accordingly, PT-112 has recently been shown to promote increases in T cell and natural killer (NK) cell proliferation in patients with recurrent thymic epithelial tumors.[5,6] Moreover, PT-112 appears to positively cooperate with various immune checkpoint inhibitors (ICIs) in syngeneic mouse tumor models.[9] In

line with this notion, Phase I and Phase IIa clinical trials testing PT-112 in combination with an ICI specific for CD274 (best known as PD-L1) documented promising activity in patients with metastatic castration-resistant prostate cancer and advanced non-small cell lung carcinoma.[2,14,15]

Of note, the ability of cancer cells to release endogenous molecules with adjuvant-like activity as they succumb to perturbations of homeostasis that cannot be resolved by core mechanisms of adaptation, such as the integrated stress response (ISR) or autophagy,[16] is critical for cell death to be perceived as immunogenic.[13,17] These molecules are commonly referred to as damage-associated molecular patterns (DAMPs) and include calreticulin (CALR), which is exposed on the surface of cancer cells undergoing ICD as a consequence of eukaryotic translation initiation factor 2 subunit alpha (EIF2S1, best known as eIF2α) phosphorylation, as well as ATP and high-mobility group box 1 (HMGB1), which are released therefrom.[18–20] Moreover, the activation of adaptive immunity by dying cells generally involves their ability to secrete immunostimulatory cytokines like type I interferon (IFN), a process that (at least in some settings) results from

mitochondrial damage and the consequent release of mitochondrial DNA (mtDNA) in the cytosol, culminating with the activation of cyclic GMP-AMP synthase (CGAS).[21,22] Finally, the effector phase of antigen-specific anticancer immune responses as elicited by ICD requires that target cells present antigenic determinants on their surface in complex with MHC Class I molecules to enable recognition and elimination by CD8^{+} cytotoxic T lymphocytes (CTLs).[23,24] Importantly, malignant cells under attack by CTLs often expose increased levels of the co-inhibitory ligand CD274 (best known as PD-L1) on their surface.[25] While *a priori* PD-L1 exposure by cancer cells limits CTL activation upon binding to programmed cell death 1 (PDCD1, best known as PD-1), it also provides a therapeutically actionable target for ICIs.[25]

Mitochondrial outer membrane permeabilization (MOMP), which is elicited by BCL2 associated X, apoptosis regulator (BAX) and BCL2 antagonist/killer 1 (BAK1) and antagonized by BCL2, apoptosis regulator (BCL2) and BCL2-like 1 (BCL2L1, best known as BCL-X_L), has been involved not only in the ability of multiple anticancer agents to kill malignant cells,[26,27] but also in their capacity to elicit the secretion of type I IFN via the mtDNA-dependent activation of CGAS.[21,28–30] Here, we harnessed mouse hormone receptor (HR)-positive TS/A cells[31] to test the implication of MOMP in the mechanism of action of PT-112. Besides recapitulating the ability of PT-112 to mediate antiproliferative and cytotoxic effects that are accompanied by *bona fide* ICD markers including CALR exposure and HMGB1 release, we found that TS/A cells responding to PT-112 exhibit eIF2α phosphorylation and cytosolic mtDNA accumulation, secrete type I IFN, and present increased levels of MHC Class I molecules and PD-L1 on their surface. Importantly, most of these effects were not abrogated by genetic alterations affecting the molecular machinery of MOMP, suggesting that PT-112 may be effective against a wide variety of malignancies, including various neoplasms that – as part of natural evolution or in response to (immuno) therapy – have lost, at least in part, MOMP competence. This is particularly relevant given that numerous (epi)genetic defects consistently associated with oncogenesis and tumor progression, such as inactivating alterations of tumor protein 53 (TP53, best known as p53) signaling (which affect >50% of solid malignancies) or genetic events resulting in BCL2 overexpression (which drive specific forms of lymphoma) directly or indirectly afford transformed cells with increased MOMP resistance.[32,33]

Materials and methods

Cell culture

Mouse mammary adenocarcinoma TS/A cells (SCC177) were purchased from Millipore Sigma. Wild-type (WT) TS/A and TS/A-derived clones were maintained in culture at 37°C and 5% of CO_2 in DMEM containing 1 mm sodium pyruvate, and 1 mm HEPES buffer, 4.5 g/L glucose (Corning®), and supplemented with 10% fetal calf serum (GeminiBio), 100 μg/mL streptomycin sulfate, 100 U/mL penicillin sodium and 290 μg/mL L-glutamine (Gibco™). To generate mitochondrial DNA (mtDNA)-depleted (rho[0]) cells, WT TS/A cells were treated with 500 ng/mL ethidium bromide (Sigma) for 10 days in complete culture medium (as above) further supplemented with 50 μg/mL uridine (Sigma) and 1 mm sodium pyruvate (Life Technologies).

CRISPR/Cas9

WT TS/A cells were transfected with a commercial control CRISPR-cas9 plasmid (CRISPR06-1EA, Sigma Aldrich) or customized CRISPR-cas9 plasmids based on CRISPR06-1EA targeting *Bak1*, *Bax*, *Bcl2*, *Bcl2l1* (Sigma Aldrich), harnessing the TransIT-CRISPR as per the manufacturer recommendation. Thereafter, individual GFP-expressing cells were sorted into 96-well plates by means of a FACS Symphony S6 Sorter (BD Biosciences), followed by clonal expansion and gene knockout validation by immunoblotting.

Immunoblotting

Immunoblotting was performed according to established protocols[21] with primary antibodies specific for BAK1 (#12105, Cell Signaling Technology, 1:500), BAX (#2772, Cell Signaling Technology, 1:1,000), BCL2 (#3498, Cell Signaling Technology, 1:500), BCL-X_L (#2764, Cell Signaling Technology, 1:500), phospho-eIF2α (Ser51) (#9721, Cell Signaling Technology, 1:500) eIF2α (#9722, Cell Signaling Technology, 1:500), and ACTB1 (#3700, Cell Signaling Technology, 1:2,000), the latter of which employed as a control of equal lane loading. PageRuler™ Plus Prestained Protein Ladder, 10–250 kDa (#26619, Thermo Fisher) was employed as molecular weight (MW) marker. After washing and incubating with horseradish peroxidase-conjugated anti-rabbit (#NA934, GE Healthcare Life Sciences, 1:5,000) or anti-mouse secondary antibodies (#NA931, GE Healthcare Life Sciences, 1:5,000), protein expression levels were visualized on an Azure 600 Imaging System operated by Azure capture v. 1.9.0.0406 (Azure Biosystems) upon membrane incubation with the SuperSignal West Femto Maximum Sensitivity Substrate (#34094, Thermo Fisher).

Cell number and cell death

Cell number and cell death were evaluated by flow cytometry using an Attune NxT flow cytometer (Thermo Fisher Scientific) upon staining with 0.5 μg/mL 4′,6-diamidino-2-phenylindole (DAPI, Sigma-Aldrich).

Clonogenic assays

When untreated colonies attained maximal plate occupancy while remaining separated from each other (generally 7–10 days), colonies were fixed with 70% ethanol and stained with 0.1% crystal violet (Electron Microscopy Sciences), as previously reported.[34] Colonies were enumerated manually by means of an eCountTM Colony counter (Heathrow Scientific).

Mitochondrial parameters

Mitochondrial transmembrane potential ($\Delta\psi_m$) and mitochondrial mass were analyzed by flow cytometry using an Attune NxT flow cytometer (Thermo Fisher Scientific) upon staining with 100 nM MitoTracker™ Deep Red FM (Invitrogen™), 150 nM of MitoTracker™ Green FM (Invitrogen™), and 0.5 µg/mL DAPI (Sigma-Aldrich), which was used as a vital dye.

DAMP emission

HMGB1, and type I IFN releases were quantified with the HMGB1 express ELISA Kit (Tecan) and the IFN-β ELISA kit, high sensitivity (PBL Assay Science), respectively, as per the manufacturer's instructions. A FlexStation 3 Multi-Mode Microplate Reader operated by SoftMaxPro v.5.4.6 (Molecular Devices LLC) was employed to measure sample absorbance at 450 nm. Absolute quantification of protein levels was calculated based on standard curves with $R^2 \geq 0.99$.

MHC-I, CRT, and PD-L1 surface expression

Cells were washed with PBS and stained with Zombie Aqua™ Fixable Viability Kit (BioLegend) for 15 min. Subsequently, cells were washed and incubated with the Calreticulin (D3E6) XP® rabbit monoclonal antibody PE Conjugate (#19780S, cell signaling, 0.5 µL/sample) and PE anti-mouse H-2 Antibody anti-H-2 - M1/42 (#125505, BioLegend, 1 µL/sample) or APC anti-mouse CD274 (B7-H1, PD-L1) (#124312, BioLegend, 0.75 µL/sample) in 0.5% BSA in PBS (FACS buffer) for 25 min at 4°C in the dark. Cells were next washed and fixed with eBioscience™ Intracellular Fixation & Permeabilization Buffer Set (Invitrogen) for 30 min at 4°C in the dark, incubated with the permeabilization buffer eBioscience™ Intracellular Fixation & Permeabilization Buffer Set (Invitrogen) for 5 min, washed, and resuspended in FACS buffer for analysis by flow cytometry (Attune NxT flow cytometer, Thermo Fisher Scientific). Zombie Aqua™ positive cells (*i.e.*, dead cells) were excluded from the analysis.

Immunofluorescence microscopy

For cytosolic dsDNA analysis, cells growing on glass coverslips were fixed with 4% paraformaldehyde (#sc -281,692, Santa Cruz Biotechnology), and plasma membranes were permeabilized with 0.1% Tween 20 and 0.01% Triton X-100 in PBS, followed by incubation with specific Anti-ds DNA antibody (#ab27156, Abcam, 1:1,000). Cells were next washed with 0.1% Tween 20 in PBS and incubated with Goat Anti-Mouse IgG H&L (Alexa Fluor® 488) pre-adsorbed (#ab150117, Abcam). Samples were eventually washed and mounted on slides with Hoechst 33,342-containing ProLong Glass Antifade Mountant (Thermo Fisher Scientific).

Images were acquired with an EVOS FL Imaging System operated by embedded software v.1.4 (Rev 26,059) (Thermo Fisher Scientific). Quantitative dsDNA analyses were performed on ≥10 randomly selected images per condition. Briefly, blue (nuclear) and green (dsDNA) levels were normalized with a LUT file optimized for each sample set on Photoshop v. 25.7.0 (Adobe), followed by the identification of nuclear and cytoplasmic regions of interest, which were quantified for the presence and relative localization of dsDNA spots above a predefined threshold size (to account for background noise) with Cell Profiler v. 4.2.1 (Broad Institute). All steps were performed with software input commands that are publicly available at https://cellprofiler. org/.[35,36]

Data processing and statistical analysis

Data processing, plotting, and statistical analysis were implemented on Prism v. 10 (GraphPad) and Excel 2021 (Microsoft). Figures were prepared on Illustrator 2020 (Adobe). Unless otherwise noted, for statistical analysis, two-way ANOVA and uncorrected Fisher's LSD were applied in comparisons involving two or more groups. For samples not following a Gaussian distribution, statistical significance was assessed by Wilcoxon test. Unless otherwise noted, all experiments were performed at least in three independent replicates.

Results

Antiproliferative and cytotoxic effects

To investigate the involvement of the molecular machinery for MOMP in the anticancer activity of PT-112, we harnessed the CRISPR/Cas9 technology to establish multiple mouse HR$^+$ mammary carcinoma TS/A cell clones lacking *Bax* and *Bak1*, or *Bcl2* and *Bcl2l1* (Supplementary Figure S1) and tested their sensitivity to the antiproliferative and cytotoxic effects of PT-112. In line with previous findings,[7–9] exposing control TS/A cells to 20 µM or 40 µM PT-112 resulted in a pronounced proliferative arrest (Figure 1(a)) coupled with a dose-dependent accumulation of dead cells (Figure 1b), as assessed by cell number enumeration via flow cytometry in the presence of a DAPI, which selectively stains dead cells.[37] Of note, while the ability of PT-112 to mediate acute cytotoxicity against TS/A cells was exacerbated in *Bcl2$^{-/-}$Bcl2l1$^{-/-}$* TS/A cell clones and compromised in *Bax$^{-/-}$Bak1$^{-/-}$* TS/A cell clones (Figure 1b), its antiproliferative potential was not altered by genetic perturbations affecting MOMP (Figure 1a). These findings were corroborated by conventional clonogenic assays[34] (Figure 1c).

Cell death driven by PT-112 in control TS/A cells was accompanied by a substantial dose-dependent increase in total mitochondrial mass (Figure 1d) and a less pronounced increase in mitochondrial transmembrane potential ($\Delta\psi_m$) (Figure 1e), as assessed by flow cytometry upon staining with the mass- and $\Delta\psi_m$-sensitive probes MitoTracker™ Green FM and MitoTracker™ Deep Red FM, respectively. Taken together, these two changes elicited by PT-112 resulted in relative (mass-normalized) mitochondrial depolarization (Figure 1f). Of note, the increase in mitochondrial mass driven by PT-112 was exacerbated in *Bcl2$^{-/-}$Bcl2l1$^{-/-}$* TS/A cell clones and reduced in *Bax$^{-/-}$Bak1$^{-/-}$* TS/A cell clones (Figure 1d), the latter of which also exhibited increased mitochondrial polarization as compared to control TS/A cells (Figure 1e). In this setting,
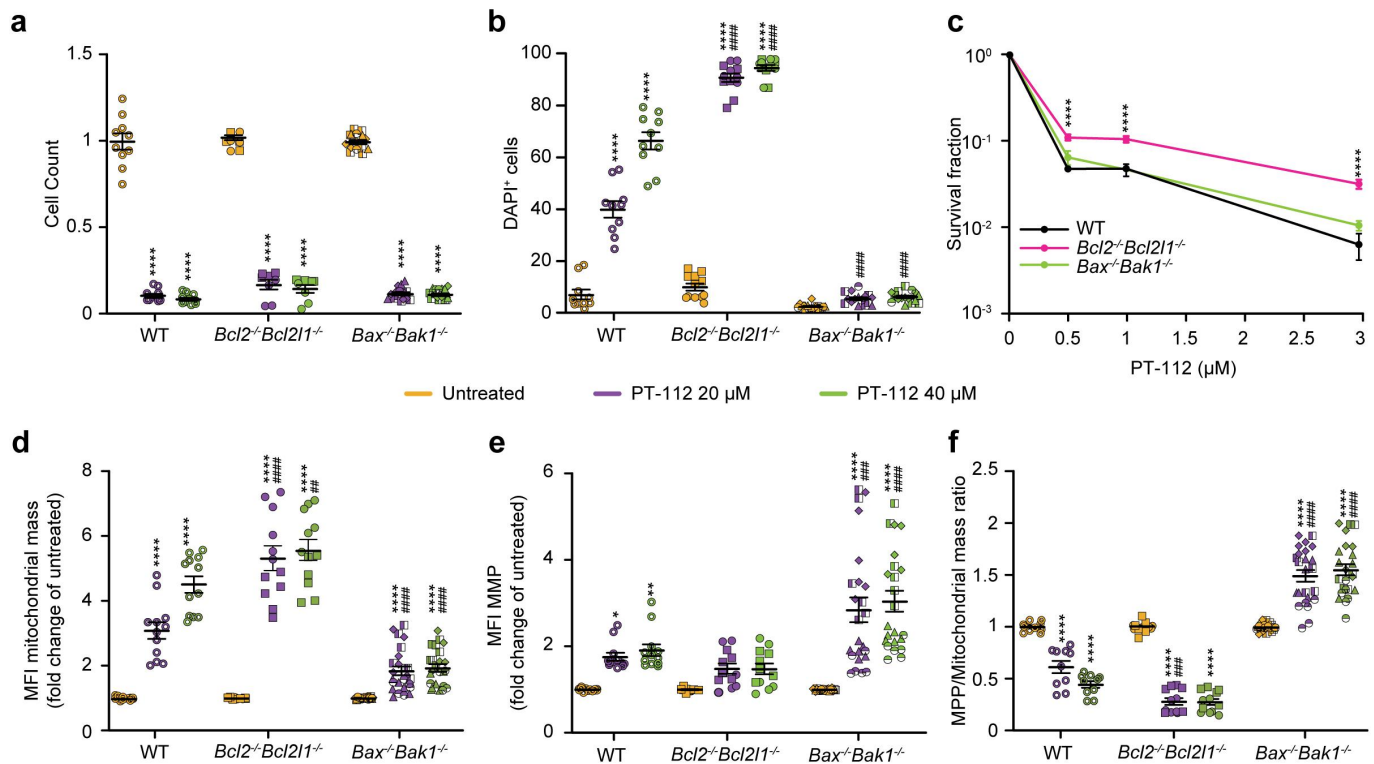
Figure 1. PT-112 mediates MOMP-dependent overt cytotoxicity but MOMP-independent antiproliferative effects. Wild-type (WT) TS/A cells or TS/A clones of the indicated genotype were optionally exposed to 20 μM or 40 μM PT-112 for 72 hrs and then processed for the flow cytometry-assisted quantification of residual viable cells (a), cell death (b), mitochondrial mass (d), mitochondrial membrane potential (MMP; e), and relative MMP (f). Alternatively, TS/A cells or TS/A clones of the indicated genotype were optionally exposed to 0.5 μM, 1 μM or 3 μM PT-112 for 72 hrs and allowed to generative colonies for 7 days (c). In A, B, D, E, and F results are means ± SEM of 2 biological duplicates from 3 independent experiments. In C, results are means ± SEM of 6 biological duplicates from at least 3 independent experiments. In A, D, E, and F, data are normalized to untreated cells of the same genotype. ****$p < 0.0001$, **$p < 0.01$, *$p < 0.05$, compared to untreated cells of the same genotype; ####$p < 0.0001$, ###$p < 0.001$, ##$p < 0.01$, compared to WT TS/A cells treated with the same dose of PT-112 (two-way ANOVA). Each symbol represents different cell clones with the same genotype. See also Supplementary Figure A1.

$Bcl2^{-/-}Bcl2l1^{-/-}$ TS/A cell clones exhibited greater relative mitochondrial depolarization in response to PT-112 compared to their control counterparts, while $Bax^{-/-}Bak1^{-/-}$ TS/A cell clones responded to PT-112 with mass-normalized mitochondrial hyperpolarization (Figure 1f). This is in line with (1) the role of MOMP and consequent mitochondrial depolarization in apoptotic cell death,[38] and (2) the differential sensitivity of $Bcl2^{-/-}Bcl2l1^{-/-}$ and $Bax^{-/-}Bak1^{-/-}$ TS/A cell clones to PT-112-induced cell death (Figure 1b).

Taken together, these findings indicate that PT-112 exerts antiproliferative effects independent of mitochondrial apoptosis but mediates overt cytotoxicity largely through BAX- and BAK1-dependent MOMP.

Immunogenicity

We next focused on the impact of the MOMP machinery on the ability of PT-112 to promote the release of ICD-relevant DAMPs and modulate the visibility of cancer cells to CD8+ CTLs.[39] The relative mitochondrial depolarization promoted by PT-112 in TS/A cells (Figure 1f) was accompanied by the accumulation of cytosolic double-stranded DNA (dsDNA) (Figure 2a,b) which is known to drive type I IFN secretion.[22] Such an increase was significantly inhibited in TS/A cells depleted of mtDNA upon long-term culture in the presence of ethidium bromide (rho⁰ cells)[40] (Figure 2c), mechanistically

demonstrating that PT-112 induces cytosolic mtDNA accumulation.

In line with this notion, TS/A cells exposed to PT-112 secreted approximately two-fold more interferon beta 1 (IFNB1) in their supernatant than their control counterparts (Figure 2d). However, while the absence of BAX and BAK1 limited cytosolic dsDNA accumulation in TS/A cells responding to PT-112 (Figure 2a,b), it did not compromise PT-112-driven type I IFN secretion (Figure 2d), potentially suggesting that PT-112 promotes type I IFN synthesis via mtDNA-independent mechanisms. Lending further support to this possibility, the $Bcl2^{-/-}Bcl2l1^{-/-}$ phenotype paradoxically limited the ability of 20 (but not 40) μM PT-112 to promote cytosolic dsDNA accumulation (Figure 2a,b), but had marginal effects on PT-112 driven type I IFN production (Figure 2d). Whether such a paradoxical impact on PT-112-driven cytosolic dsDNA accumulation reflects the MOMP-dependent hyperactivation of mitophagy, a specific variant of autophagy that disposes of permeabilized (and hence mtDNA-releasing) mitochondria, in $Bcl2^{-/-}Bcl2l1^{-/-}$ cellular systems[41] remains to be determined.

As previously demonstrated with higher PT-112 doses,[9] WT TS/A cells exposed to 20 μM or 40 μM PT-112 for 48 hours exposed CALR on the outer leaflet of the plasma membrane, with no sizable differences across doses (Figure 3a), an immunogenic effect that was not influenced by the $Bax^{-/-}Bak1^{-/-}$ or
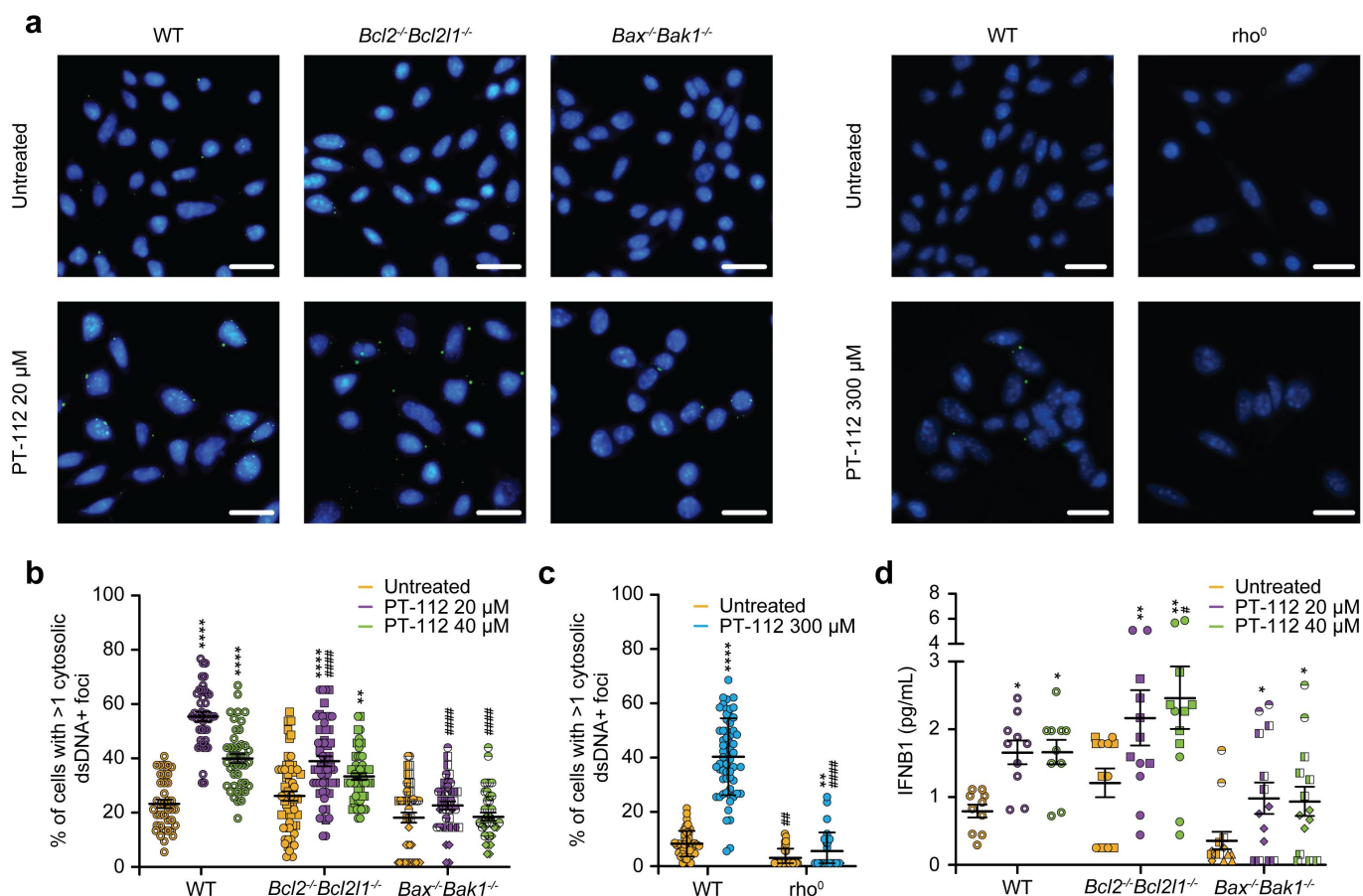
Figure 2. PT-112 elicits MOMP-dependent cytosolic dsDNA accumulation, but MOMP-independent type I IFN secretion. Wild-type (WT) TS/A cells, rho[0] TS/A cells, or TS/A clones of the indicated genotype/phenotype were optionally exposed to the indicated concentration of PT-112 for 72 (a,b) or 24 (c,d) hrs and then processed for the immunofluorescence microscopy-assisted quantification of cytosolic double-stranded DNA (dsDNA; A,B,C) or the ELISA-based quantification of IFNB1 secretion in the culture supernatant (d). In A, representative images are reported, scale bar: 20 μm. In B,C, results are means ± SEM of 3 biological duplicates from 2 independent experiments. In D, results are means ± SEM of 2 biological duplicates from 3 independent experiments. ****$p < 0.0001$, **$p < 0.01$, *$p < 0.05$, compared to untreated cells of the same genotype; ####$p < 0.0001$, ##$p < 0.01$, #$p < 0.05$, compared to WT TS/A cells treated with the same dose of PT-112 (paired two-tailed Student's t-test). Each symbol represents different cell clones with the same genotype.

the $Bcl2^{-/-}Bcl2l1^{-/-}$ genotype (Figure 3a). These findings are in line with the notion that CALR exposure in malignant cells undergoing ICD involves the ISR, and notably its pathognomonic inactivating phosphorylation of eukaryotic translation initiation factor 2 subunit alpha (EIF2S1, best known as eIF2α), but not MOMP.[39] Indeed, exposing WT TS/A cells to a high-dose PT-112 challenge resulted in rapid eIF2α phosphorylation non-linearly increasing over time up to 24 hours (Figure 3b). PT-112 also elicited the exposure of the co-inhibitory ligand PD-L1 on the surface of TS/A cells in a dose dependent but MOMP-independent manner (Figure 3c), which is in line with the fact that PD-L1 exposure on cancer cells normally does not involve MOMP.[25]

At odds with previous findings obtained with ~100 μM PT-112,[9] WT TS/A cells treated *in vitro* with 20 μM or 40 μM PT-112 for 48 hours did not release significant amounts of HMGB1 in the culture supernatant (Figure 3d). Conversely, the concomitant absence of BCL2 and BCL-X$_L$ enabled abundant HMGB1 secretion by TS/A cell clones responding to PT-112, which is in line with the accrued cytotoxic response of these cells (Figure 1b). $Bax^{-/-}Bak1^{-/-}$ TS/A cell clones exposed to 40 μM PT-112 for 48 hours exhibited significantly reduced HMGB1 release as compared to their similarly treated WT

counterparts, although the magnitude of this effect was minimal (Figure 3d). Most likely, such a marginal effect was due to the lack of substantial HGMB1 release in WT TS/A cells. Finally, TS/A cells exposed to 20 μM or 40 μM PT-112 for 48 hours also exhibited a nearly 2-fold upregulation in surface-exposed MHC Class I molecules as compared to their untreated counterparts, an immunogenic shift that was not consistently affected by the co-deletion of *Bcl2* and *Bcl2l1* or *Bax* and *Bak1* (Figure 3e).

Altogether, our findings point to a minor involvement of the molecular machinery for MOMP in the ability of PT-112 to elicit the emission of ICD-relevant DAMPs by TS/A cells and increase their visibility to immune effector cells.

Discussion

In summary, the molecular machinery for MOMP is involved in the overt cytotoxic effects that PT-112 exerts on mouse HR$^+$ mammary carcinoma TS/A cells (Figure 1b) and the consequent release of the immunostimulatory DAMP HMGB1 (Figure 3d), but it appears to be dispensable for PT-112 anti-proliferative effects (Figure 1a,c). Moreover, while defects in the molecular machinery for MOMP may promote the
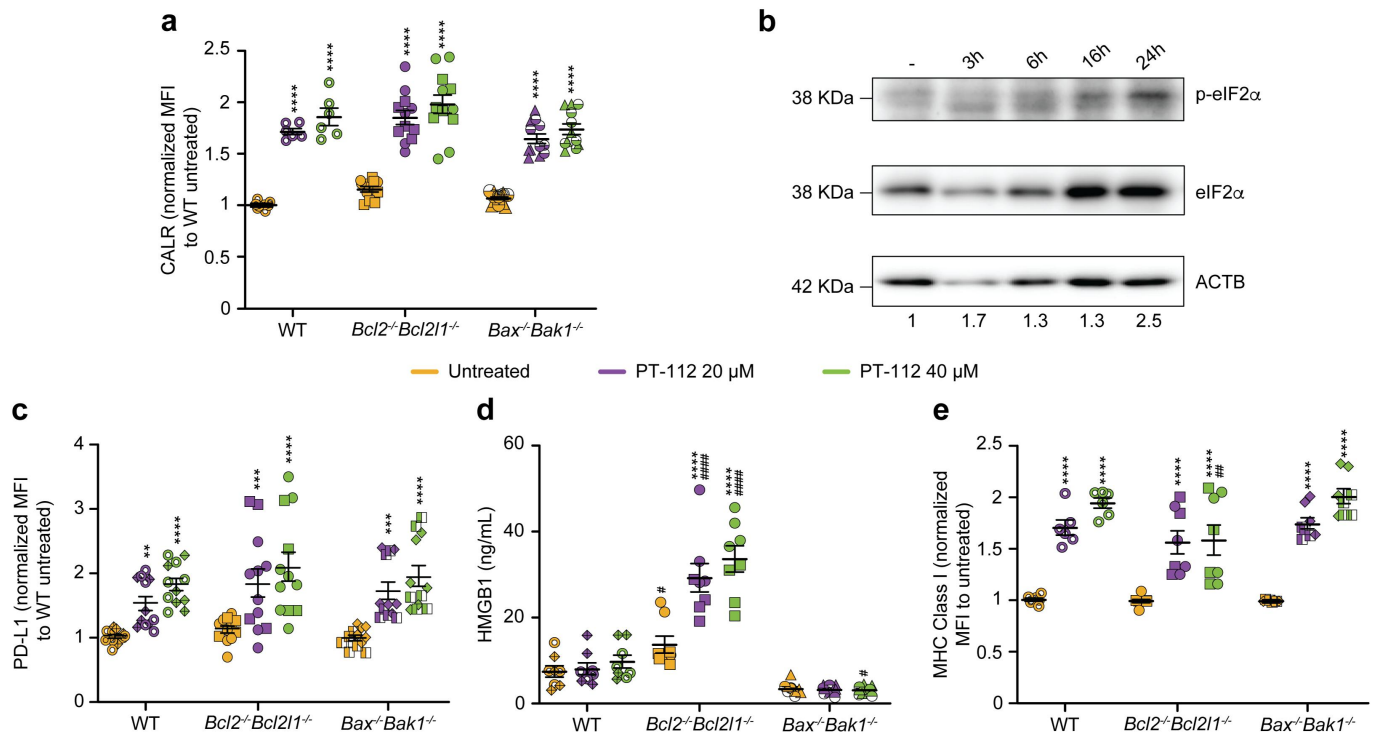
Figure 3. PT-112 drives MOMP-independent CALR, MHC class I and PD-L1 exposure on the plasma membrane, but MOMP-dependent HGMB1 secretion. Wild-type (WT) TS/A cells or TS/A cell clones of the indicated genotype were optionally exposed to the indicated concentrations of PT-112 (~600 μM, when not specified) for (up to) 48 hrs and processed for the flow cytometry-assisted quantification of CALR (a), PD-L1 (c) or MHC Class I (e) exposure on the plasma membrane, the immunoblotting-assisted assessment of elf2α phosphorylation (b), or the ELISA-based quantification of HGMB1 release in the culture supernatant (d). In A,C-E, results are means ± SEM of 2 biological duplicates from 3 independent experiments. In A,C,E, data are normalized to untreated WT cells (a,c) or untreated cells of the same genotype (e) upon exclusion of dead (DAPI⁻) cells from the analysis. In B, representative immunoblotting images are reported, numbers indicate relative densitometric abundance upon normalization to total ACTB levels in control conditions. ****$p < 0.0001$, ***$p < 0.001$, **$p < 0.01$, compared to untreated cells of the same genotype; ####$p < 0.0001$, ##$p < 0.01$, #$p < 0.05$, compared to WT TS/A cells treated with the same dose of PT-112 (two-way ANOVA). Each symbol represents different cell clones with the same genotype.

resistance of malignant cells to ICD-driven anticancer immunity as executed by CD8⁺ T cells,[17] they do not suppress the ability of PT-112 to elicit the ICD-related exposure of CALR, MHC Class I molecules and PD-L1 on the surface of TS/A cells (Figure 3a,c,e). Finally, while the concomitant absence of BAX and BAK1 limited the cytosolic accumulation of mtDNA in TS/A cells as elicited by PT-112, the co-deletion of *Bcl2* and *Bcl2l1* had a paradoxical inhibitory effect on this process, at least when PT-112 was employed at 20 μM (Figure 2b). Along similar lines, the *Bcl2⁻/⁻Bcl2l1⁻/⁻* genotype conferred a (marginal, but statistically significant) paradoxical advantage to TS/A cells responding to low-dose PT-112 and assessed for residual clonogenic potential (Figure 1c). These findings may indicate that TS/A cells lacking *Bcl2* and *Bcl2l1* are particularly prone to undergo mitophagy,[41] a specific variant of autophagy that efficiently degrades permeabilized (and hence apoptosis-initiating and mtDNA-releasing) mitochondria.[42,43] Thus, it will be interesting to test the ability of PT-112 to elicit mtDNA accumulation and to limit clonogenic potential in *Bcl2⁻/⁻Bcl2l1⁻/⁻* TS/A cells co-exposed to autophagy inhibitors such as the lysosome-targeting agents chloroquine and hydroxychloroquine.[44]

Activation of apoptotic caspases as elicited by widespread MOMP has been associated with multipronged immunosuppressive effects including suppressed type I IFN signaling in a variety of settings.[45–47] At least hypothetically, this may also explain why *Bcl2⁻/⁻Bcl2l1⁻/⁻* TS/A cells (which are more prone to

activate caspases as compared to their WT counterparts) failed to exhibit superior type I IFN secretion in response to PT-112 (Figure 2d). Whether increased caspase activation might also explain why the overt cytotoxic effects of PT-112 in WT TS/A cells exhibited a clear dose-dependency (Figure 1b), but 20 μM PT-112 was superior to 40 μM PT-112 at eliciting cytosolic dsDNA accumulation in the same cellular system (Figure 2b) remains to be formally investigated.

Of note, while *Bax⁻/⁻Bak1⁻/⁻* TS/A cells exhibited limited PT-112-driven cytosolic dsDNA accumulation as compared to their WT counterparts (Figure 2b), the concomitant absence of BAX and BAK1 failed to affect PT-112-drive type I IFN secretion, possibly pointing to extramitochondrial nucleic acids (notably nuclear DNA or RNA species) as potential drivers of the latter process. Additional work is required to clarify this possibility. Finally, it will be interesting to assess the implication of other molecules that interact with the core MOMP machinery in the cytotoxic and immunogenic effects of PT-112, for instance, by co-exposing *Bcl2⁻/⁻Bcl2l1⁻/⁻* TS/A cells to PT-112 plus an inhibitor of MCL1 apoptosis regulator, BCL2 family member (MCL1) such as ABBV-467,[48] or *Bax⁻/⁻Bak1⁻/⁻* TS/A cells to PT-112 plus a mitochondrial permeability transition (MPT) inhibitor such as cyclosporin A (CsA).[49]

In summary, besides confirming the ability of PT-112 to induce the emission of multiple ICD-relevant DAMPs, the present findings demonstrate the ability of PT-112 to drive

the secretion of type I IFN, MHC Class I presentation and compensatory PD-L1 exposure in TS/A cells independent of MOMP functionality. Thus, the molecular machinery for MOMP appears to be only partially involved in the cytotoxicity and immunogenicity of PT-112, suggesting that this agent may be active in a variety of tumors exhibiting MOMP defects.

Author contributions

CRediT: **Ruth Soler-Agesta:** Investigation, Writing – review & editing; **Manuel Beltrán-Visiedo:** Investigation, Writing – review & editing; **Ai Sato:** Investigation; **Takahiro Yamazaki:** Investigation; **Emma Guilbaud:** Investigation; **Christina Y. Yim:** Writing – review & editing; **Maria T. Congenie:** Writing – review & editing; **Tyler D. Ames:** Conceptualization, Writing – review & editing; **Alberto Anel:** Writing – review & editing; **Lorenzo Galluzzi:** Conceptualization, Writing – original draft, Writing – review & editing.

Disclosure statement

CYY, MTC and TDA are full-time employees of Promontory Therapeutics. RS-A has been sponsored by Promontory Therapeutics and Asociación Española Contra el Cáncer (AECC). LG is/has been holding research contracts with Lytix Biopharma, Promontory Therapeutics and Onxeo, has received consulting/advisory honoraria from Boehringer Ingelheim, AbbVie, AstraZeneca, OmniSEQ, Onxeo, The Longevity Labs, Inzen, Imvax, Sotio, Promontory, Noxopharm, EduCom, and the Luke Heller TECPR2 Foundation, and holds Promontory Therapeutics stock options. All other authors have no conflicts to declare.

ORCID

Ruth Soler-Agesta http://orcid.org/0000-0003-3153-389X
Manuel Beltrán-Visiedo http://orcid.org/0000-0002-7977-8020
Alberto Anel http://orcid.org/0000-0002-5175-8394
Lorenzo Galluzzi http://orcid.org/0000-0003-2257-8500

Data availability statement

Data and materials supporting the results or analyses presented in their paper are available upon reasonable request.

References

1. Karp DD, Camidge DR, Infante JR, Ames TD, Price MR, Jimeno J, Bryce AH. Phase I study of PT-112, a novel pyrophosphate-platinum immunogenic cell death inducer, in advanced solid tumours. EClinicalMedicine. 2022;49:101430. doi: 10.1016/j.eclinm.2022.101430.

2. Bryce AH, Dronca RS, Costello BA, Aparicio A, Subudhi SK, O'Donnell JF, Jimeno J, Yim CY, Ames TD, Price M, et al. A phase 1b study of novel immunogenic cell death inducer PT-112 plus PD-L1 inhibitor avelumab in metastatic castrate-resistant prostate cancer (mCRPC) patients. J Clin Oncol. 2021;39(15_suppl):e17025–e17025. doi: 10.1200/JCO.2021.39.15_suppl.e17025.

3. Bryce AH, Dronca RS, Costello BA, Infante JR, Ames TD, Jimeno J, Karp DD. PT-112 in advanced metastatic castrate-resistant prostate cancer (mCRPC), as monotherapy or in combination with PD-L1 inhibitor avelumab: findings from two phase I studies. J Clin Oncol. 2020;38(6_suppl):83–83. doi: 10.1200/JCO.2020.38.6_suppl.83.

4. Bryce AH, Karp DD, Tagawa ST, Nordquist LT, Rathkopf DE, Adra N, Dorff TB, Baeck J, O'Donnell JF, Ames TD, et al. A phase 2 study of immunogenic cell death inducer PT-112 in patients with metastatic castration-resistant prostate cancer. J Clin Oncol. 2023;41(6_suppl):TPS292–TPS292. doi: 10.1200/JCO.2023.41.6_suppl.TPS292.

5. McAdams M, Swift S, Donahue RN, Celades C, Tsai Y-T, Bingham M, Szabo E, Zhao C, Sansone S, Choradia N, et al. Preliminary efficacy, safety, and immunomodulatory effects of PT-112 from a phase 2 proof of concept study in patients (pts) with thymic epithelial tumors (TETs). J Clin Oncol. 2023;41 (16_suppl):e20647–e20647. doi: 10.1200/JCO.2023.41.16_suppl.e20647.

6. McAdams M, Swift S, Donahue RN, Celades C, Tsai Y-T, Bingham M, Szabo E, Zhao C, Sansone S, Feierabend C, et al. AB016. Phase 2 clinical trial of PT-112 in patients with thymic epithelial tumors. Mediastinum. 2023;7:AB016–AB016. doi: 10.21037/med-23-ab016.

7. Ames T, Slusher B, Wozniak K, Takase Y, Shimizu H, Nishibata-Kobayashi K, Kanada-Sonobe RM, Kerns W, Fong KL, Pourquier P, et al. Findings across pre-clinical models in the development of PT-112, a novel investigational platinum-pyrophosphate anti-cancer agent. Eur J Public Health Cancer. 2016;69:S153–S153. doi: 10.1016/S0959-8049(16)33054-4.

8. Soler-Agesta R, Moreno-Loshuertos R, Yim CY, Congenie MT, Ames TD, Johnson HL, Stossi F, Mancini MG, Mancini MA, Ripollés-Yuba C, et al. Cancer cell-selective induction of mitochondrial stress and immunogenic cell death by PT-112 in human prostate cell lines. J Transl Med. 2024;22(1):927. doi: 10.1186/s12967-024-05739-x.

9. Yamazaki T, Buque A, Ames TD, Galluzzi L. PT-112 induces immunogenic cell death and synergizes with immune checkpoint blockers in mouse tumor models. Oncoimmunology. 2020;9 (1):1721810. doi: 10.1080/2162402X.2020.1721810.

10. Yim CY, Congenie MT, Johnson HL, Mancini MG, Stossi F, Mancini MA, Azofeifa J, Price MR, Baeck J, Ames TD. Abstract C128: PT-112, a novel immunogenic cell death inducer, causes ribosomal biogenesis inhibition and organelle stress in cancer cells. Mol Cancer Ther. 2023;22(12_Supplement):C128–C128. doi: 10.1158/1535-7163.TARG-23-C128.

11. Soler-Agesta R, Marco-Brualla J, Minjárez-Sáenz M, Yim CY, Martínez-Júlvez M, Price MR, Moreno-Loshuertos R, Ames TD,

Jimeno J, Anel A. PT-112 induces mitochondrial stress and immunogenic cell death, targeting tumor cells with mitochondrial deficiencies. Cancers (Basel). 2022;14(16):3851. doi: 10.3390/cancers14163851.

12. Yamazaki T, Ames TD, Galluzzi L. Abstract B199: potent induction of immunogenic cell death by PT-112. Cancer Immunol Res. 2019;7(2_Supplement):B199–B199. doi: 10.1158/2326-6074.CRICIMTEATIAACR18-B199.

13. Kroemer G, Galassi C, Zitvogel L, Galluzzi L. Immunogenic cell stress and death. Nat Immunol. 2022;23(4):487–500. doi: 10.1038/s41590-022-01132-2.

14. Imbimbo M, Ghisoni E, Mulvey A, Bouchaab H, Mederos Alfonso N, Karp D, Camidge DR, Mansfield AS, Yim CY, Ames TD, et al. 125P a phase IIa study of the novel immunogenic cell death (ICD) inducer PT-112 plus avelumab ("PAVE") in advanced non-small cell lung cancer (NSCLC) patients (pts). Immuno-Oncol Technol. 2022;16:100237. doi: 10.1016/j.iotech.2022.100237.

15. Karp DD, Dronca RS, Camidge R, Costello BA, Mansfield AS, Ames TD, Jimeno JM, Bryce AH. 1026MO phase ib dose escalation study of novel immunogenic cell death (ICD) inducer PT-112 plus PD-L1 inhibitor avelumab in solid tumours. Ann Oncol. 2020;31:S708–S708. doi: 10.1016/j.annonc.2020.08.1146.

16. Galluzzi L, Yamazaki T, Kroemer G. Linking cellular stress responses to systemic homeostasis. Nat Rev Mol Cell Biol. 2018;19(11):731–745. doi: 10.1038/s41580-018-0068-0.

17. Galassi C, Chan TA, Vitale I, Galluzzi L. The hallmarks of cancer immune evasion. Cancer Cell. 2024;42(11):1825–1863. doi: 10.1016/j.ccell.2024.09.010.

18. Fucikova J, Spisek R, Kroemer G, Galluzzi L. Calreticulin and cancer. Cell Res. 2021;31(1):5–16. doi: 10.1038/s41422-020-0383-9.

19. Kepp O, Bezu L, Yamazaki T, Di Virgilio F, Smyth MJ, Kroemer G, Galluzzi L. ATP and cancer immunosurveillance. EMBO J. 2021;40(13):e108130. doi: 10.15252/embj.2021108130.

20. De Martino M, Rathmell JC, Galluzzi L, Vanpouille-Box C. Cancer cell metabolism and antitumour immunity. Nat Rev Immunol. 2024;24(9):654–669. doi: 10.1038/s41577-024-01026-4.

21. Yamazaki T, Kirchmair A, Sato A, Buqué A, Rybstein M, Petroni G, Bloy N, Finotello F, Stafford L, Navarro Manzano E, et al. Mitochondrial DNA drives abscopal responses to radiation that are inhibited by autophagy. Nat Immunol. 2020;21(10):1160–1171. doi: 10.1038/s41590-020-0751-0.

22. Marchi S, Guilbaud E, Tait SWG, Yamazaki T, Galluzzi L. Mitochondrial control of inflammation. Nat Rev Immunol. 2023;23(3):159–173. doi: 10.1038/s41577-022-00760-x.

23. Jhunjhunwala S, Hammer C, Delamarre L. Antigen presentation in cancer: insights into tumour immunogenicity and immune evasion. Nat Rev Cancer. 2021;21(5):298–312. doi: 10.1038/s41568-021-00339-z.

24. Yang K, Halima A, Chan TA. Antigen presentation in cancer — mechanisms and clinical implications for immunotherapy. Nat Rev Clin Oncol. 2023;20(9):604–623. doi: 10.1038/s41571-023-00789-4.

25. Yamaguchi H, Hsu JM, Yang WH, Hung MC. Mechanisms regulating PD-L1 expression in cancers and associated opportunities for novel small-molecule therapeutics. Nat Rev Clin Oncol. 2022;19(5):287–305. doi: 10.1038/s41571-022-00601-9.

26. Tait SW, Green DR. Mitochondria and cell death: outer membrane permeabilization and beyond. Nat Rev Mol Cell Biol. 2010;11(9):621–632. doi: 10.1038/nrm2952.

27. Bock FJ, Tait SWG. Mitochondria as multifaceted regulators of cell death. Nat Rev Mol Cell Biol. 2020;21(2):85–100. doi: 10.1038/s41580-019-0173-8.

28. McArthur K, Whitehead LW, Heddleston JM, Li L, Padman BS, Oorschot V, Geoghegan ND, Chappaz S, Davidson S, San Chin H, et al. BAK/BAX macropores facilitate mitochondrial herniation and mtDNA efflux during apoptosis. Science. 2018;359(6378). doi: 10.1126/science.aao6047.

29. Riley JS, Quarato G, Cloix C, Lopez J, O'Prey J, Pearson M, Chapman J, Sesaki H, Carlin LM, Passos JF, et al. Mitochondrial inner membrane permeabilisation enables mtDNA release during apoptosis. EMBO J. 2018;37(17). doi: 10.15252/embj.201899238.

30. Vanpouille-Box C, Hoffmann JA, Galluzzi L. Pharmacological modulation of nucleic acid sensors — therapeutic potential and persisting obstacles. Nat Rev Drug Discov. 2019;18(11):845–867. doi: 10.1038/s41573-019-0043-2.

31. De Giovanni C, Nicoletti G, Landuzzi L, Palladini A, Lollini P-L, Nanni P. Bioprofiling TS/A murine mammary cancer for a functional precision experimental Model. Cancers (Basel). 2019;11(12):1889. doi: 10.3390/cancers11121889.

32. Hanahan D. Hallmarks of cancer: new dimensions. Cancer Discov. 2022;12(1):31–46. doi: 10.1158/2159-8290.CD-21-1059.

33. Hanahan D, Weinberg RA. Hallmarks of cancer: the next generation. Cell. 2011;144(5):646–674. doi: 10.1016/j.cell.2011.02.013.

34. Serrano-Mendioroz I, Garate-Soraluze E, Rodriguez-Ruiz ME. A simple method to assess clonogenic survival of irradiated cancer cells. Methods Cell Biol. 2023;174:127–136.

35. Sato A. Quantification of cytosolic DNA species by immunofluorescence microscopy and automated image analysis. Methods Cell Biol. 2022;172:115–134.

36. Sato A, Buque A, Yamazaki T, Bloy N, Petroni G, Galluzzi L. Immunofluorescence microscopy-based assessment of cytosolic DNA accumulation in mammalian cells. STAR Protoc. 2021;2(2):100488. doi: 10.1016/j.xpro.2021.100488.

37. Galluzzi L, Aaronson SA, Abrams J, Alnemri ES, Andrews DW, Baehrecke EH, Bazan NG, Blagosklonny MV, Blomgren K, Borner C, et al. Guidelines for the use and interpretation of assays for monitoring cell death in higher eukaryotes. Cell Death Differ. 2009;16(8):1093–1107. doi: 10.1038/cdd.2009.44.

38. Vitale I, Pietrocola F, Guilbaud E, Aaronson SA, Abrams JM, Adam D, Agostini M, Agostinis P, Alnemri ES, Altucci L, et al. Apoptotic cell death in disease—current understanding of the NCCD 2023. Cell Death Differ. 2023;30(5):1097–1154. doi: 10.1038/s41418-023-01153-w.

39. Galluzzi L, Guilbaud E, Schmidt D, Kroemer G, Marincola FM. Targeting immunogenic cell stress and death for cancer therapy. Nat Rev Drug Discov. 2024;23(6):445–460. doi: 10.1038/s41573-024-00920-9.

40. Soler-Agesta R. Generation of transmitochondrial cybrids in cancer cells. Methods Cell Biol. 2024;189:23–40.

41. Lindqvist LM, Heinlein M, Huang DC, Vaux DL. Prosurvival bcl-2 family members affect autophagy only indirectly, by inhibiting Bax and Bak. Proc Natl Acad Sci USA. 2014;111(23):8512–8517. doi: 10.1073/pnas.1406425111.

42. Vargas JNS, Hamasaki M, Kawabata T, Youle RJ, Yoshimori T. The mechanisms and roles of selective autophagy in mammals. Nat Rev Mol Cell Biol. 2023;24(3):167–185. doi: 10.1038/s41580-022-00542-2.

43. Galluzzi L, Morselli E, Vicencio J, Kepp O, Joza N, Tajeddine N, Kroemer G. Life, death and burial: multifaceted impact of autophagy. Biochem Soc Trans. 2008;36(5):786–790. doi: 10.1042/BST0360786.

44. Galluzzi L, Bravo-San Pedro JM, Levine B, Green DR, Kroemer G. Pharmacological modulation of autophagy: therapeutic potential and persisting obstacles. Nat Rev Drug Discov. 2017;16(7):487–511. doi: 10.1038/nrd.2017.22.

45. Rodriguez-Ruiz ME, Buqué A, Hensler M, Chen J, Bloy N, Petroni G, Sato A, Yamazaki T, Fucikova J, Galluzzi L. Apoptotic caspases inhibit abscopal responses to radiation and identify a new prognostic biomarker for breast cancer patients. Oncoimmunology. 2019;8(11):e1655964. doi: 10.1080/2162402X.2019.1655964.

46. Rongvaux A, Jackson R, Harman CD, Li T, West A, de Zoete M, Wu Y, Yordy B, Lakhani S, Kuan C-Y, et al. Apoptotic caspases prevent the induction of type I interferons by mitochondrial DNA. Cell. 2014;159(7):1563–1577. doi: 10.1016/j.cell.2014.11.037.

47. White MJ, McArthur K, Metcalf D, Lane R, Cambier J, Herold M, van Delft M, Bedoui S, Lessene G, Ritchie M, et al. Apoptotic caspases suppress mtDNA-induced STING-mediated type I IFN production. Cell. 2014;159(7):1549–1562. doi: 10.1016/j.cell.2014.11.036.

48. Yuda J, Will C, Phillips DC, Abraham L, Alvey C, Avigdor A, Buck W, Besenhofer L, Boghaert E, Cheng D, et al. Selective MCL-1 inhibitor ABBV-467 is efficacious in tumor models but is associated with cardiac troponin increases in patients. Commun Med (Lond). 2023;3(1):154. doi: 10.1038/s43856-023-00380-z.

49. Bonora M, Giorgi C, Pinton P. Molecular mechanisms and consequences of mitochondrial permeability transition. Nat Rev Mol Cell Biol. 2022;23(4):266–285. doi: 10.1038/s41580-021-00433-y.